Drug Development and Industrial Pharmacy, 33:667–676, 2007

ISSN: 0363-9045 print / 1520-5762 online
DOI: 10.1080/03639040600943814

informa
healthcare

Mechanistic Study on Hydration and Drug Release Behavior of Sodium Alginate Compacts

Lai Wah Chan, Ai Ling Ching, Celine Valeria Liew and Paul Wan Sia Heng
Department of Pharmacy, Faculty of Science, National University of Singapore, Singapore

ABSTRACT The influence of sodium alginate viscosity on the dynamics of matrix hydration, solvent front movement, swelling, erosion, and drug release from alginate matrix tablets were examined. The solvent front showed preferential penetration from the radial direction even though matrix swelling showed axial predominance. This study proposed alternative views for the anisotropic behavior of hydrating alginate compacts, namely, formation of gel barrier with different permeability characteristics, tension at the gel-core interface and preferential radial erosion, in addition to an in-depth examination on the contribution of stress relaxation of hydrated polymer as well as core expansion. Alginate matrices demonstrated pH-dependent hydration, swelling and erosion behavior, resulting in pH-dependent drug release mechanisms. Dissolution profiles for alginate matrices of different viscosities were similar in acid but differed upon increase of pH. This was due to the influence of alginate viscosity grade on liquid uptake, erosion and pronounced swelling at near neutral pH.

KEYWORDS Alginate, Solvent penetration front, Viscosity, Anisotropy, Dimensional changes

INTRODUCTION

Compressed hydrophilic matrices are widely used as modified release dosage forms for oral drug delivery. Much attention has been accorded to studying the drug release mechanism from such systems, particularly matrices compressed from hypromellose. The drug release phenomenon from hydrophilic matrices is multifaceted. Upon contact with aqueous medium, solvent hydrates the matrix surface, forming a gel barrier, which regulates solvent ingress and drug release. Further solvent imbibition into the matrix leads to matrix bulk hydration and drug dissolution, followed by matrix swelling and erosion. Moreover, the glassy-to-rubbery transition of polymer beyond a critical solvent concentration leads to changes in volume, concentration and diffusion coefficients of the involved species (Siepmann & Peppas, 2000). Ultimately, the drug release profiles from such matrices are controlled by the

Address correspondence to Paul Wan Sia Heng, Department of Pharmacy, Faculty of Science, National University of Singapore, 18 Science Drive 4, Singapore 117543, Singapore; E-mail: phapaulh@nus.edu.sg

rate of matrix hydration, swelling, drug diffusion through the gel layer and matrix erosion (Roy & Rohera, 2002). The presence of additives may also influence the time-dependent microstructure of the matrix during release. For example, addition of water soluble components may increase the porosity of the matrix during dissolution. For pH sensitive polymers such as sodium alginate, effect of pH has to be considered since it would influence polymer solubility and matrix hydration behavior.

Sodium alginate is used to form matrix in drug delivery systems, such as beads, microspheres and matrix tablets. The naturally occurring alginates are linear unbranched polysaccharides consisting of different proportions of β-D-mannuronic acid (M) and α-L-guluronic acid (G) units. The M and G monomers are 1→4 linked by glycosidic bonds, forming homopolymeric MM or GG blocks, which are interspersed with heteropolymeric MG or GM blocks. The presence of pendent acidic groups that can accept or release protons in response to pH changes makes alginate pH-sensitive. At pH below the pKa of M (3.38) and G (3.65) monomers, the soluble sodium alginate is converted to insoluble alginic acid (Haug, 1964), resulting in changes in the characteristics of the gel barrier formed, which in turn affects drug release across this barrier. Hodsdon et al. (1995) reported that a "viscous and soluble" gel barrier was formed at neutral pH, whereas a "tough, rubbery rind" was observed at acidic pH, and this difference in gel barrier property was postulated to lead to differing drug release kinetics at acidic and neutral pH.

Although sodium alginate has a long history of use, the hydration kinetics of sodium alginate compacts is not well characterized since alginates are usually formulated and studied as microcapsules, beads and films or membranes. In the development of matrix systems, it is useful to know which mass transport phenomena contribute to drug release. The most important rate-controlling mechanisms in drug release are diffusion, swelling and erosion (Kanjickal & Lopina, 2004). Tahara et al. (1995) postulated that the rate limiting mechanism for the release of a highly water soluble drug is the rate of solvent penetration, whereas the release of drugs with poor aqueous solubility is dependent on matrix erosion. In addition, Colombo et al. (1995) reported that solvent transport process into swellable polymer matrices and the corresponding dimensional changes had a major influence on drug release from these matrices. Hence, this study aims to characterize solvent penetration into alginate matrices and the corresponding dimensional changes at different pH, using two viscosity grades of sodium alginates. Compacts were also assessed for their gravimetric liquid uptake and erosion, with respect to their release properties.

MATERIALS AND METHODS

Materials

Two grades of sodium alginate, Manucol LB and Manucol SS/LL (ISP-Alginates Industries, San Diego, CA), cryogenically milled to similar median particle sizes, were used as matrix forming material, and each had kinematic viscosities of 3 and 108 mm^2/s (for 1% w/w alginate solution in water at 37°C), respectively. The model drug used, chlorpheniramine maleate (BP grade, China), which has high aqueous solubility that is relatively similar at both acidic and neutral pH (650 and 584 g/L at pH 1.2 and 6.8, respectively, at 37°C) ensures that drug release is primarily dependent on the properties of the matrix and not on drug solubility. Methylene blue was used as a marker for liquid penetration into the matrix.

Preparation of Matrix Tablets

Sodium alginate (304.5 mg/tablet) and chlorpheniramine maleate (40 mg/tablet), with or without methylene blue (2 mg/tablet), were mixed, followed by addition of magnesium stearate as lubricant (3.5 mg/tablet) and further mixing, before being compressed into 350 ± 5 mg tablets at porosity levels of 0.2 to 0.25 using a single-punch machine (F3, Manesty) with 9.5 mm diameter flat punches. Thicker matrices of similar composition were also made. The matrix tablets were stored in a desiccator for at least 3 days to allow for tablet relaxation before use.

Matrix Hydration and In Vitro Drug Release

Matrix hydration and drug release studies were evaluated using USP Method A (chapters <711> and <724>) at 50 rpm and 37 ± 0.5°C with paddles (USP Apparatus II, Vankel, Edison, NJ). Dissolution test was first carried out in 750 mL of 0.1*N* hydrochloric

acid (pH 1.2) for 2 hr and pH of the medium was then adjusted to 6.8 by adding 250 mL of 0.2*M* sodium phosphate solution, preheated to 37°C. Either 2*M* hydrochloric acid or 2*M* sodium hydroxide was used for minor adjustment of the pH of the dissolution media when necessary. Each matrix tablet was placed on a stainless steel mesh to prevent matrix-vessel adhesion while allowing unrestricted matrix swelling and free-access of medium to the entire matrix.

For drug release evaluation, matrices with and without methylene blue were used and the release profiles were compared to check for potential matrix-dye interaction. Results showed that dye addition did not influence drug release behavior of alginate matrices. Aliquot solutions were collected at suitable time intervals and assayed spectrophotometrically (Shimadzu, UV-1201, Kyoto, Japan) at 266 and 262 nm for samples in acid and buffer, respectively, using the appropriate Beer's plots. For each formulation, at least triplicate dissolution runs were carried out.

Measurement of Liquid Transport by Gravimetry and Image Analysis

At appropriate time intervals, hydrated matrices were retrieved from the dissolution vessels, gently blotted to remove excess medium and weighed. The change in matrix weight was calculated using Eq. (1):

$$\%\ \text{Weight change} = 100 \times (W_w - W_i)/W_i \qquad (1)$$

where W_w and W_i are the wet and initial weights of the matrix, respectively.

The matrices were then immersed in liquid nitrogen for 5–10 s to prevent matrix deformation upon cutting and halt liquid movement for accurate determination of matrix and hydrated layer dimensions. This freezing time hardened the external gel layer without completely freezing the matrix, which would otherwise fracture upon cutting. Comparison of matrix dimensions before and after freezing showed that cryo-treatment of matrix tablets did not affect axial or radial swelling profiles of alginate matrices. The partially frozen matrices were then sectioned axially with a sharp blade. Images of cross-sectioned matrices were captured with a digital camera (E-300, Olympus Imaging, Tokyo, Japan) and analyzed using an imaging software (Image-Pro Plus, Media Cybernetics, Silver Spring, MD). The hydrated layer was stained blue and the dry core appeared yellowish with specks of dark blue particles. At least three matrices were measured for each time point. For each matrix, the dimensions of the entire matrix, dry core and hydrated layer were measured in the axial and radial directions. Matrix swelling was expressed as a percentage of the initial diameter or thickness of the matrix; aspect ratio was calculated as the ratio of swollen tablet diameter to swollen tablet height; and hydrated layer thickness as well as core dimension were the actual dimension of the colored layer and the core, respectively.

Matrix Erosion

At suitable time intervals, the matrices were removed from the hydration medium and oven-dried at 60°C to constant weight. The extent of matrix erosion was calculated using Eq. (2):

$$\%\ \text{Matrix erosion} = 100 \times (W_i - W_d)/W_i \qquad (2)$$

where W_i and W_d are the initial and the final dry weights of the matrix, respectively.

Liquid uptake per unit weight of matrix remaining was also calculated at each time point to account for the effect of matrix erosion. Hence, liquid uptake per unit weight of matrix remaining was computed according to the following Eq. (3):

$$\%\ \text{Liquid uptake} = 100 \times (W_w - W_d)/W_d \qquad (3)$$

Curve Fitting and Statistical Analysis

The profiles of liquid uptake, swelling, hydrated area (%) and drug release were curve-fitted to zero order and Higuchi's square root equations. Dissolution profiles were compared using similarity factor, f_2, and the profiles were significantly different if $f_2 < 50$.

RESULTS AND DISCUSSION

Hydration Behavior of Alginate Matrices

Liquid Uptake and Matrix Erosion

Profiles of weight change in the acid phase were similar for both Manucol LB and Manucol SS/LL

matrices (Fig. 1). Following pH change, a sudden increase in weight change (%) was observed for Manucol SS/LL matrices, followed by a more gradual increase, whereas a rapid decline in weight occurred with Manucol LB matrices. This observation corresponded with matrix erosion results (Fig. 2), which showed rapid erosion of Manucol LB matrices in the buffer phase. When liquid uptake was corrected for matrix erosion (Fig. 1), Manucol LB matrices showed 12% higher uptake in acid (not reflected in graph due to scale) and exponential increase in liquid uptake in the buffer phase, whereas Manucol SS/LL matrices showed a more linear trend (note that the last point for Manucol LB was near complete erosion). The faster initial liquid uptake of Manucol LB matrices compared to Manucol SS/LL matrices (61.9 ± 2.4 and 48.6 ± 3.9, respectively at 15 min) could indicate more rapid hydration of lower viscosity alginate prior to the formation of an acid gel barrier. After the initial spurt in uptake, both matrices showed similar hydration rates, and liquid uptake was linear with square root time ($R^2 > 0.96$).

Liquid uptake was higher in the buffer phase for both types of matrices compared to the acid phase. At pH 6.8, alginic acid was converted to anionic alginate molecules. High ion concentration within the matrix due to deprotonation of acidic groups and diffusion of counter ions from the surrounding medium enhanced liquid imbibition into the matrix via osmosis, resulting in increased swelling (Fig. 3) described by the Donnan equilibrium (Brondsted & Kopecek, 1992). Liquid uptake in buffer occurred linearly for both matrices and only up to 5 hr for Manucol LB matrices (the last time point was ignored due to near-complete matrix dissolution).

Matrix erosion was less than 20% in the acid phase (less than 16% if corrected for drug loss) and increased with time in the buffer phase (Fig. 2). At low pH, the acid gel was relatively resistant to erosion as it was insoluble. At pH 6.8, alginate becomes soluble and more susceptible to erosion, the extent of which depends on the molecular weight of the polymer. Longer polymer chains form stronger polymer networks due to greater extent of polymer entanglement.

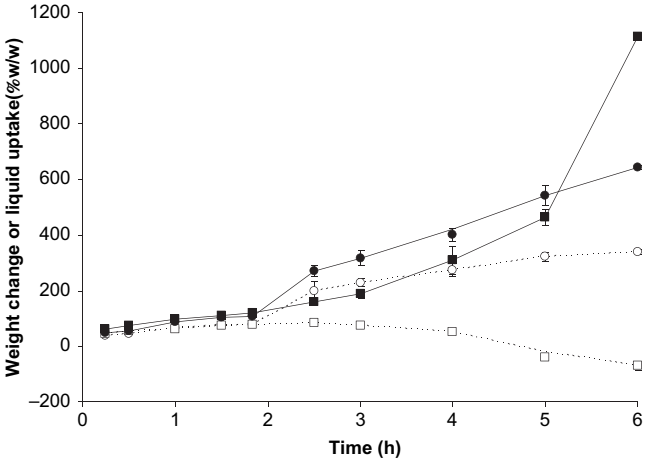

FIGURE 1 **Profiles of Percent Weight Change (Dotted Lines) and Percent Liquid Uptake Per Unit Weight Matrix Remaining (Solid Lines) for Manucol SS/LL (○, ●) and Manucol LB (□, ■) Matrices. Vertical Bars Represent Standard Deviations.**

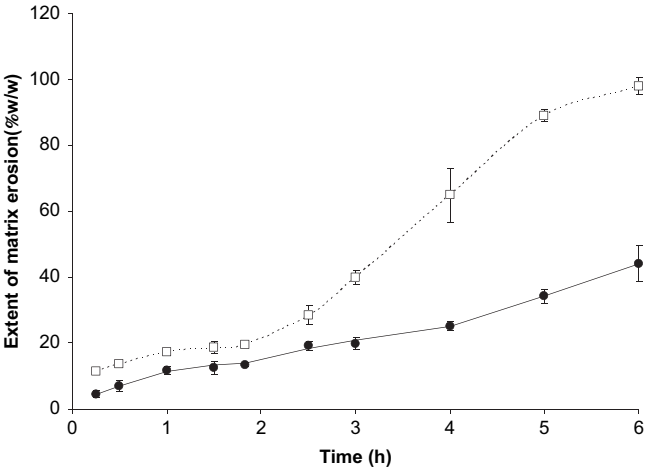

FIGURE 2 **Extent of Matrix Erosion of Manucol SS/LL (●) and Manucol LB (□) Matrices. Vertical Bars Represent Standard Deviations.**

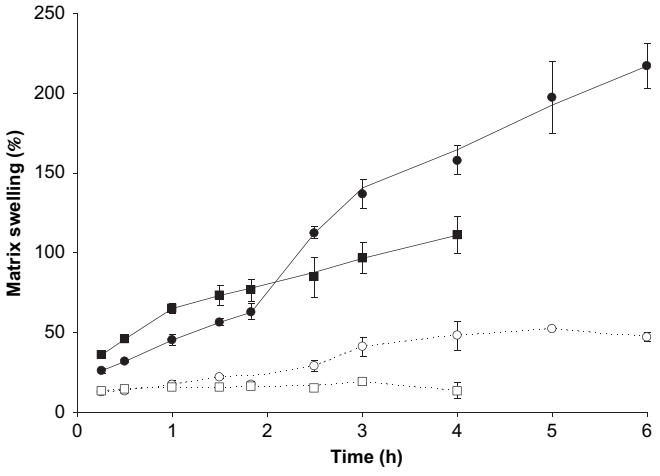

FIGURE 3 **Axial (Solid Lines) and Radial (Dotted Lines) Swelling (Relative to Initial Matrix Dimension) of Manucol SS/LL (○, ●) and Manucol LB (□, ■) Matrices. Vertical Bars Represent Standard Deviations.**

As the gel layer becomes more dilute, and the 'disentanglement concentration' is reached, the polymer chains forming the matrix disentangle and diffuse into the surrounding medium. The disentanglement concentration has been shown to decrease as the molecular weight of a polymer increases (Kavanagh & Corrigan, 2004). Hence, Manucol LB matrices showed greater erosion than Manucol SS/LL matrices due to the lower disentanglement concentration of Manucol SS/LL alginate. This meant that Manucol SS/LL polymer hydrated more extensively before its polymer chains disentangled. Manucol SS/LL matrices hydrated 600% while Manucol LB matrices hydrated 188% to produce 40% matrix erosion (Figs. 1 and 2).

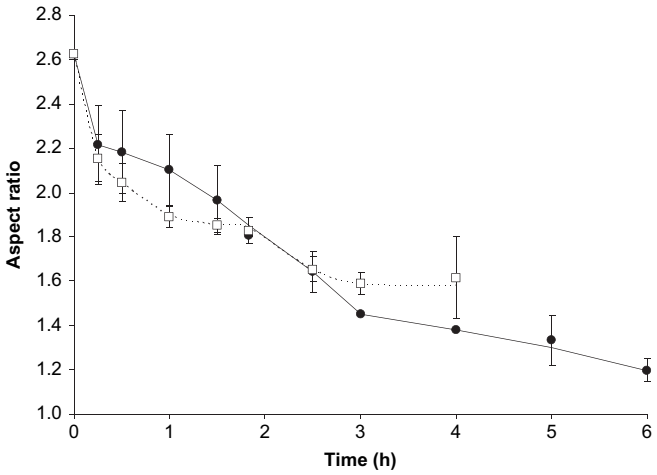

FIGURE 4 **Change in Aspect Ratio of Manucol SS/LL (●) and Manucol LB (□) Matrices with Time. Vertical Bars Represent Standard Deviations.**

Dimensional Changes

Matrix swelling was anisotropic, with preferential swelling in the axial direction (Fig. 3). Preferential axial swelling was attributed to the relief of stresses induced during compaction (Papadimitriou et al., 1993). Manucol LB matrices showed higher axial swelling in the acid phase and this corresponded to the higher acid uptake per unit weight matrix remaining for Manucol LB matrices. Radial swelling for both types of matrices were similar and remained approximately constant in the acid phase. Upon pH increase, Manucol SS/LL matrices continued to swell further in both axial and radial directions due to enhanced liquid uptake coupled with low erosion rates. Enhanced polymer relaxation in the buffer phase relative to the acid phase was also attributed to the interaction and repulsion of charges along the anionic polymer chain (Brondsted & Kopecek, 1992). In contrast, Manucol LB matrices showed slower axial growth in the buffer phase without much change in radial dimensions up to approximately 4 hr, after which, an intact core was no longer present due to extensive matrix dissolution. Wan et al. (1995) explained that higher molecular weight chains when hydrated, due to the larger hydrodynamic volume, caused greater swelling with matrices containing higher molecular weight polymers. The extent of matrix swelling was also due to a balance of liquid uptake and matrix erosion, as shown in this study. Axial swelling in the acid phase was linear with square root time while swelling in buffer phase followed zero order kinetics ($R^2 > 0.98$).

Aspect ratio was plotted against time to show the evolution in matrix morphology during hydration (Fig. 4). In general, aspect ratio decreased with time due to predominant axial swelling, moving towards a value of one, which reflects increasing sphericity. This suggested that the alginate particles, which were roughly globular in shape, had a tendency to regain spherical symmetry during hydration of the matrices (Malveau et al., 2002). However, the gradual development of hydrating matrices into a spherical shape is a more complex phenomenon, which could involve an interplay of various factors as described below.

At the interface between the planar and radial surfaces, liquid penetration was from both axial and radial directions. This ensured much higher hydration and erosion rates at the edges. In addition, as the compressed alginate particles swelled upon hydration, their collective expansion force in the larger axial front caused a strain in the gel layer. This strain produced a tension in the gel layer that favored greater expansion in the center, to ease the expansion pressures and caused a convex shaped gel layer to develop.

Given that the surface area of both axial surfaces was greater than that of the radial surface (Table 1), more solvent is expected to penetrate from the axial surfaces, potentially causing higher extent of swelling in the axial direction. This postulation was tested by comparing the swelling behavior of matrices of different initial thickness made to similar porosities (Table 1) in acidic medium. Hydration at pH 1.2 was carried out for 18 hr to ensure complete hydration of both types of matrices. Both types of matrices were found to exhibit preferential axial swelling and similar extent of

TABLE 1 **Influence of Axial and Radial Surface Area on Directional Swelling**

Type of matrix	Thickness (mm)	Diameter (mm)	Aspect ratio	Surface area (mm^2)	
				Axial	Radial
Thin	3.7	10.0	2.7	149.4	111.8
Thick	10.6	10.2	1.0	160.3	333.3

radial swelling despite differences in initial axial and radial surface areas. If surface area had an influence on the extent of directional swelling, the larger radial surface area relative to the axial surface area of the thicker tablets would have resulted in greater radial swelling. The fact that axial swelling was still greater than radial swelling in both thick and thin matrices suggested that hydrating compacts had a propensity for preferential axial expansion in the direction opposite to the compression force. These factors collectively contribute to the propensity of a wetted matrix to progress towards an increasingly spherical outline with time while undergoing dissolution.

Image Analysis of Cross-Sectioned Matrices

Matrix cross-sections revealed gradual solvent ingress indicated by a distinct dye front (Fig. 5), which reached the core at around 3 hr. Hence, this part of the study only focused on results obtained in the acid phase (0–2 hr). The percent hydrated area (indicated by the darker region in Fig. 5) relative to the entire cross-sectional area increased with time and was slightly higher for Manucol LB matrices (Fig. 6). The larger hydration area of Manucol LB matrices paralleled the higher liquid uptake observed with these matrices in the acid phase (with an average difference

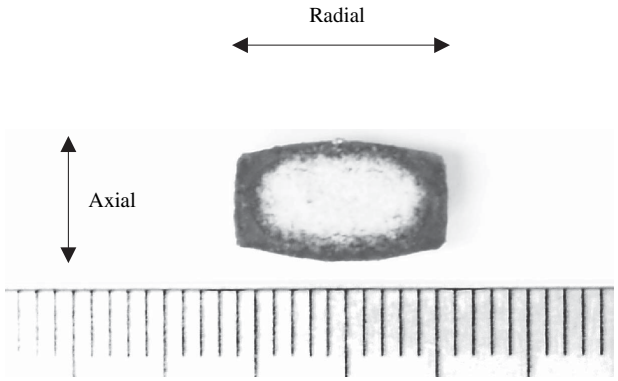

FIGURE 5 **Axial Cross-Section Image of Alginate Matrix Hydrated for 1.5 hr. Scale: 1 division=1 mm.**

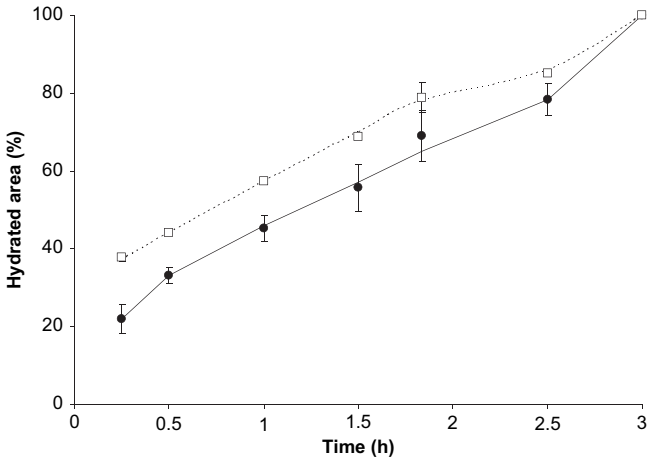

FIGURE 6 **Hydrated Area Relative to Matrix Cross-Sectional Area at Different Time Points for Manucol SS/LL (●) and Manucol LB (□) Matrices. Vertical Bars Represent Standard Deviations.**

of 12% for both parameters). With shorter chain lengths, the mobility of macromolecules increases, leading to greater free volume (Streubel et al., 2000) which enabled higher solvent diffusion into Manucol LB matrices. The increase in percent hydrated area in acid was linear with square root time ($R^2 > 0.98$), indicating dominant Fickian influence in liquid penetration.

The thickness of the hydration layer was measured in the axial and radial directions. Interestingly, the hydrated layer thickness in the radial direction was greater than that in the axial direction (Fig. 7a). This was particularly surprising since matrix axial swelling was greater than radial swelling (Fig. 3). Moreover, gel

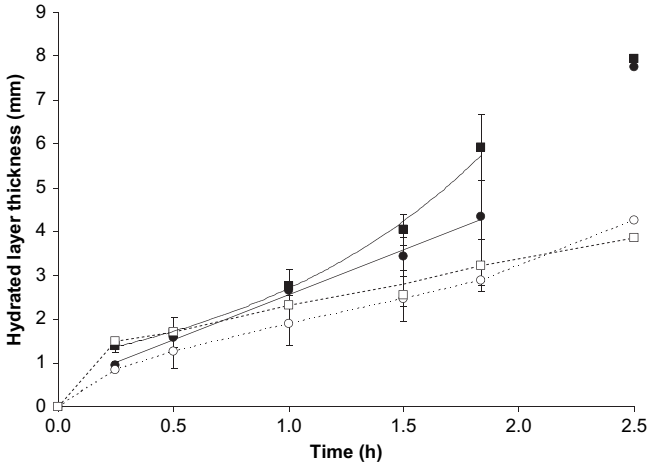

FIGURE 7a Thickness of Hydrated Layer Measured in Axial (Dotted Lines) and Radial (Solid Lines) Directions for Manucol SS/LL (○, ●) and Manucol LB (□, ■) Matrices. Vertical Bars Represent Standard Deviations.

thickness was reported to be similar in both axial and radial directions (Moussa et al., 1998). Several mechanisms could have resulted in this scenario; (i) greater axial core expansion, (ii) hindered liquid diffusion in the axial direction due to formation of a less permeable barrier, (iii) easier liquid penetration in the radial direction through laminates formation, (iv) preferential radial erosion and, and (v) predominant expansion of hydrated alginate particles in the direction of compression.

In order to determine whether core expansion played a role in the apparent difference in the axial and radial hydrated layer thickness, the dimensions of the residual dry core were subsequently measured in the radial and axial directions. Decreasing radial core diameter with time corresponding to the increase in radial hydrated layer thickness, suggested approximately constant solvent diffusion rate from the radial direction under acidic conditions (Fig. 7b). However, the axial dry core height did not change appreciably to be in tandem with the liquid front imbibing in the axial direction. In view of greater axial swelling of the entire matrix, the slower increase in axial hydrated layer thickness coupled with the almost constant axial core height could be partly attributed to axial core expansion, which opposed axial solvent front movement towards the matrix center. This was shown by a slight increase in core dimension during initial hydration (Fig. 7b). Initial axial core expansion was more conspicuous for Manucol SS/LL matrices compared to Manucol LB matrices, because of less hindered initial axial liquid front movement (Fig. 7a) into Manucol LB matrices due to its lower gel viscosity. Even with radial core expansion, liquid penetration from the sides was still more rapid. Hence, radial core expansion could only be a transient phenomenon arising from residual elastic strain in the compacts.

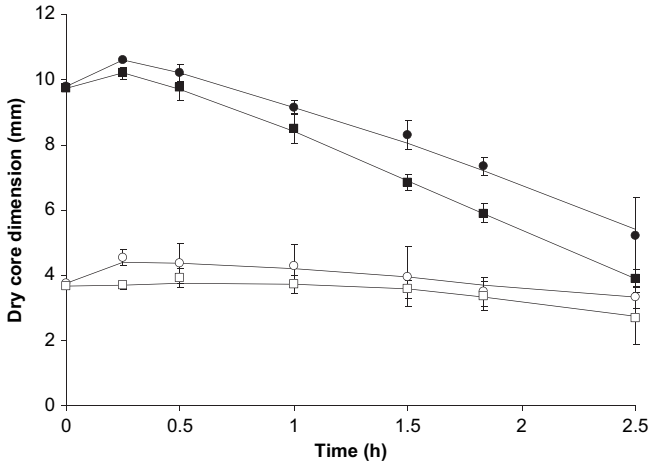

FIGURE 7b Dimensions of Residual Dry Core Measured in the Axial (Dotted Lines) and Radial (Solid Lines) Direction for Manucol SS/LL (○, ●) and Manucol LB (□, ■) Matrices. Vertical Bars Represent Standard Deviations.

Although it had been suggested that the slower apparent liquid diffusion front movement from the axial direction was due to a simultaneous axial core expansion, which opposed axial solvent front movement towards the matrix center for a relaxed aged matrix, this contribution may not be as significant. Once the compression pressure is removed and the matrix ejected from the die, an instantaneous elastic recovery results in both axial and radial directions, followed by a slower anelastic strain recovery. Eventually, only irrecoverable plastic strain remained in the matrix (Goldhoff, 1971). Evidences obtained did not strongly support this theory as alginate matrices compressed to various porosities showed rather similar dissolution profiles (Liew et al., 2006). Should the proposed core expansion be valid hindrance to liquid diffusion, it would be expected that denser compacted matrices showed slower drug release rates. This, however, was not found to be the case. Further, it had been reported that axial elastic recovery of compacts increased with increasing compaction pressure (Alderborn & Nyström, 1984). Hence, with decreasing matrix porosity, axial core expansion is expected to increase, opposing liquid movement to greater extents. Nonetheless, Rajabi-Siahboomi et al. (1994) and Moussa et al. (1998) have observed matrix core expansion phenomenon. This discrepancy could be due to the difference in gel barrier characteristics, as well as contribution from other phenomena, as explained below.

By the dynamics of compaction, volume change was largely in the axial direction. Thus, particulates undergoing compaction, especially alginate particles, experienced greater compression force in the axial orientation than radial direction and are expected to result into disc shaped plastically deformed polymeric masses within the compact. By forming a more continuous gel layer, the flattened alginate particles were capable of collectively forming a less permeable liquid penetration barrier in the axial direction. Further, liquid penetration in the axial direction retarded, resulting in slow decrease in the axial dry core dimension. In contrast, the radial direction allowed better liquid

permeation via laminates formed by stacking of axially compacted alginate particles. Evidence of this phenomenon can be seen by the occasional development of horizontal cracks or lamination on alginate matrices undergoing dissolution in the acid phase.

As liquid ingress into the core from the axial front was impeded, continued hydration of the wetted layer resulted in its gradual growth due to gel swelling, which paralleled the absolute increase in overall axial dimension. Even though the polymer particles had been plastically deformed, upon hydration, the increase in macromolecular mobility might allow polymer chains to regain their original molecular orientation, which is probably the preferred orientation. Colombo et al. (1992) provided further evidence for the propensity of matrices to swell mainly in the direction of compression. In this study, hypromellose matrices were partially coated with an impermeable film, on either the axial surface and/or the radial surface followed by immersion in a hydrating medium. The swollen matrices showed preferential axial expansion even when both axial surfaces were coated. Hence, predominant axial expansion was still observed even when liquid penetration was prevented in the axial direction.

Sitting in the dissolution vessel with the axial direction of the matrix aligned with the paddle shaft, it is expected that the circumferential region of the matrix experienced the swirling dissolution media more intensely and the tangential shear force contributed by this swirling motion aided gel erosion. Thus, radial gel erosion was expected to proceed at a higher rate than erosion from the planar surface. Although it is not possible to quantitatively determine the relative contributions by both gel fronts to matrix erosion, circumstantial evidence supported a higher radial gel erosion rate. With faster thinning of the radial gel diffusion layer, the solvent front is expected to proceed at a higher rate in the radial direction, contributing both to changing aspect ratio (Fig. 4) as well as core dimensions (Fig. 7b).

Studies have used the apparent gel front as a proxy for the apparent solvent penetration front (Gao et al., 1996). This was possible because the apparent gel front was found to be synchronized to the true solvent penetration front (Gao & Meury, 1996). However, the apparent gel front lagged behind the solvent penetration front because glassy-to-rubbery transition of the polymer only takes place when the solvent concentration threshold value is reached.

The method used in this present study, which involved the incorporation of a dye into alginate matrices, allowed direct determination of the apparent solvent penetration front since the dye front followed the solvent penetration front closely. Moreover, the extent of alginate matrix erosion in the acid phase was limited. The hydrated layer thickness in the radial direction can be used to represent the apparent solvent penetration distance in acid since radial swelling was approximately constant with time. The trend obtained showed that solvent penetration occurred linearly into Manucol SS/LL matrices and exponentially into Manucol LB matrices (Fig. 7a). The equations describing the aforementioned trends were $Y = 0.0343\ X + 0.499$ and $Y = 1.0976\ e^{0.0149X}$, respectively ($R^2 > 0.99$), where Y is the solvent penetration front in mm and X is time of hydration in minutes. This did not agree with the results from liquid uptake, swelling and hydrated area measurements. However, these three parameters take into consideration liquid penetration from all directions while radial solvent penetration distance was only measured from the radial direction. The discrepancy in solvent penetration kinetics indicated possible dissimilar solvent penetration in axial and radial directions, which could be attributed to the anisotropic behavior of matrices during dissolution. The faster radial liquid penetration in Manucol LB matrices was due to its lower acid gel viscosity. Circumferential erosion by the swirling dissolution medium caused faster surface remodeling and the dissipation of swollen gel matrix by erosion assisted in the development of a less compact gel layer. In addition, the swirling dissolution medium around the circumferential region of the matrix imparted some gentle centrifugal pull on the radial gel layer, which was more likely to affect the lower viscosity gel formed by Manucol LB alginate. These effects manifested with the marginally less hindered liquid penetration in the radial direction to bring about the observed exponential growth in the measured radial hydrated layer with time (Fig. 7a) for Manucol LB matrices. For Manucol SS/LL matrices, the higher viscosity gel layer did not respond to the small but perceptible environmental influences on the dissolving matrix and the hydrated layer developed in a linear manner, both in the axial and radial fronts.

Drug Release from Alginate Matrices

The drug release profiles of Manucol LB and Manucol SS/LL matrices in pH 1.2 followed by pH 6.8

media are shown in Fig. 8. Dissolution behavior in acid was similar for both grades of alginates. However, upon a change in pH, drug release from both types of matrices proceeded at different rates.

As mentioned earlier, Manucol LB matrices showed marginally higher liquid uptake per unit weight matrix remaining, matrix erosion and axial swelling (Figs. 1, 2, and 3) compared to Manucol SS/LL matrices in acid phase. Evidently, alginate viscosity had an effect on all these parameters but these differences did not result in significantly different (f_2=84) drug release profiles in the acid phase. In addition, the percent burst releases were similar for both matrices despite the faster initial hydration of Manucol LB matrices, as indicated by the greater burst in liquid uptake. Hence, the marginal difference in the hydration behavior of both types of matrices did not significantly influence drug release in the acid phase. Evidently, the establishment of the insoluble alginic acid layer had negated the differences in viscosity grades of the alginates.

In the buffer phase, drug release was twice as slow for Manucol SS/LL matrices as it was for Manucol LB matrices (0.11 and 0.24%/min, respectively). The extent of matrix erosion from Manucol LB matrices was much higher than Manucol SS/LL matrices (Fig. 2) and was completely eroded at the end of the experiment due to shorter chain lengths of Manucol LB, which disentangled and dissolved more readily. Matrix erosion resulted in reduced matrix dimension in both axial and radial directions and decreased diffusion path-length for drug molecules, giving rise to higher release rates. On the other hand, increased retention of the viscous swollen gel layer of Manucol SS/LL matrices increased diffusion path-length of the drug. Hence, drug release in the buffer phase was dependent on alginate viscosity, which influenced the swelling and erosion behavior of the matrices.

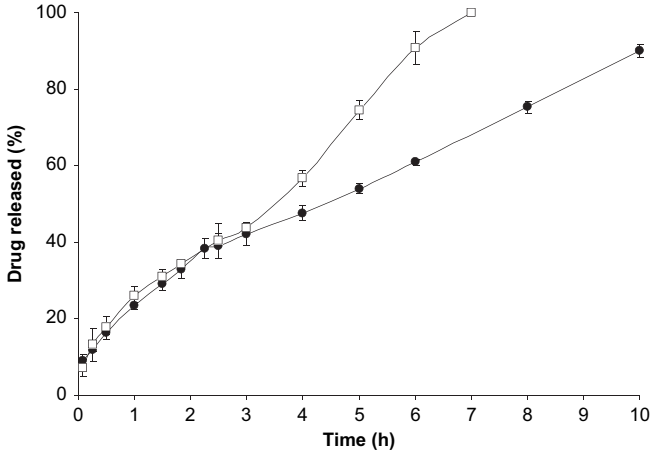

FIGURE 8 **Drug Release Profiles from Manucol SS/LL (●) and Manucol LB (□) Matrices. Vertical Bars Represent Standard Deviations.**

Curve fitting studies showed that drug release in the acid phase followed Higuchi's square root of time model and the percent drug release became linear with time upon pH change ($R^2 > 0.99$). Hence, drug was released predominantly by Fickian diffusion in acid and was erosion or swelling-controlled in the buffer phase. This was expected since surface sodium alginate was converted to insoluble alginic acid, which showed limited swelling, liquid uptake and erosion in the acid phase. Therefore, drug was predominantly released via diffusion through the alginic acid gel barrier. Upon pH change, alginic acid was reconverted to soluble sodium alginate, which showed greater swelling, liquid uptake and erosion. Zero order release can be attributed to either a case II transport (swelling- or relaxation-controlled system) or an erosion-controlled system. For Manucol LB matrices, erosion was more likely to predominate while both erosion and swelling contributed to release from Manucol SS/LL matrices in buffer.

CONCLUSION

The pH-responsive characteristic of the alginate polymer gave rise to different hydration, swelling and erosion kinetics at acidic and near-neutral pH, resulting in pH-dependent drug release. Matrix hydration in acid followed Fickian kinetics and was swelling/erosion-controlled in buffer, similar to the drug release kinetics. The influence of alginate viscosity on matrix behavior was dominant when alginate is in its soluble ionic form. In its insoluble form, alginate viscosity had marginal influence on matrix hydration behavior and did not significantly influence drug release in the acid phase. This allows the use of different viscosity grade alginates to obtain the desired release profile in the buffer phase without changing the release profile in acid. Close examination of anisotropic matrix behavior during hydration suggests that the hydration of alginate compacts is a complex phenomenon involving the interaction of various factors. The nonuniform manner in which solvent diffuses into the matrix could imply nonuniform drug release from different parts of the matrix.

A better understanding of matrix behavior during dissolution study could be elucidated by observing the extent and pattern of liquid penetration with the aid of a dye.

REFERENCES

Alderborn, G., & Nyström, C. (1984). Radial and axial tensile strength and strength variability of paracetamol tablets. *Acta Pharm. Suec.*, *21*, 1–8.

Brondsted, H., & Kopecek, J. (1992). pH-sensitive hydrogels. In *Polyelectrolyte Gels: Properties, Preparation and Applications;* Harland, R.S., & Prud'homme, R.K., Ed.; American Chemical Society: Washington, DC, 285–304.

Colombo, P., Bettini, R., Massimo, G., Catellani, P. L., & Peppas, N. A. (1995). Drug diffusion front movement is important in drug-release control from swellable matrix tablets. *J. Pharm. Sci., 84,* 991–997.

Colombo, P., Catellani, P. L., Peppas, N. A., Maggi, L., & Conte, U. (1992). Swelling characteristics of hydrophilic matrices for controlled-release: new dimensionless number to describe the swelling and release behavior. *Int. J. Pharm., 88,* 99–109.

Gao, P., & Meury, R. H. (1996). Swelling of hydroxypropyl methylcellulose matrix tablets. 1. Characterization of swelling using a novel optical imaging method. *J. Pharm. Sci., 85,* 725–731.

Gao, P., Skoug, J. W., Nixon, P. R., Ju, T. R., Stemm, N. L., & Sung, K.-C. (1996). Swelling of hydroxypropyl methylcellulose matrix tablets. 2. Mechanistic study of the influence of formulation variables on matrix performance and drug release. *J. Pharm. Sci.*, *85*, 732–740.

Goldhoff, R. M. (1971). Creep recovery in heat resistant steels. In *Advances in Creep Design, the A. E. Johnson Memorial Volume*; Smith, A.I., & Nicolson, A.M., Eds.; Applied Science Publishers: London, 81–109.

Haug, A. (1964). Composition and properties of alginates. Thesis. Norweigian institute of Technology, Trondheim.

Hodsdon, A. C., Mitchell, J. R., Davies, M. C., & Melia, C. D. (1995). Structure and behavior in hydrophilic matrix sustained release dosage forms: 3. The influence of pH on the sustained-release performance and internal gel structure of sodium alginate matrices. *J. Control. Release*, *33*, 143–152.

Kanjickal, D. G., & Lopina, S. T. (2004). Modeling of drug release from polymeric delivery systems-A review. *Crit. Rev. Ther. Drug.*, *21*, 345–386.

Kavanagh, N, & Corrigan, O. I. (2004). Swelling and erosion properties of hydroxypropylmethylcellulose (Hypromellose) matrices –influence of agitation rate and dissolution medium composition. *Int. J. Pharm.*, *279*, 141–152.

Liew, C. V., Chan, L. W., Ching, A. L., & Heng, P. W. S. (2006). Evaluation of sodium alginate as drug release modifier in matrix tablets. *Int. J. Pharm.*, *309*, 25–37.

Malveau, C., Baille, W. E., Zhu, X. X., & Marchessault, R. H. (2002). NMR imaging of high-amylose starch tablets. 2. Effect of tablet size. *Biomacromolecules*, *3*, 1249–1254.

Moussa, I. S., Lenaerts, V., & Cartilier, L. H. (1998). Image analysis studies of water transport and dimensional changes occurring in the early stages of hydration in cross-linked amylase matrices, *J. Control. Release*, *52*, 63–70.

Papadimitriou, E., Buckton, G., & Efentakis, M. (1993). Probing the mechanisms of swelling of hydroxypropylmethylcellulose matrices. *Int. J. Pharm.*, *98*, 57–62.

Rajabi-Siahboomi, A. R., Bowtell, R. W., Mansfield, P., Henderson, A., Davies, M. C., & Melia C. D. (1994). Structure and behaviour in hydrophilic matrix sustained release dosage forms: 2. NMR-imaging studies of dimensional changes in the gel layer and core of HPMC tablets undergoing hydration. *J. Control. Release*, *31*, 121–128.

Roy, D. S., Rohera, B. D. (2002). Comparative evaluation of rate of hydration and matrix erosion of HEC and HPC and study of drug release from their matrices. *Eur. J. Pharm. Sci.*, *16*, 193–199.

Siepmann, J., & Peppas, N. A. (2000). Hydrophilic matrices for controlled drug delivery: an improved mathematical model to predict the resulting drug release kinetics (the "Sequential Layer" model). *Pharm. Res.*, *17*, 1290–1298.

Streubel, A., Siepmann, J., Peppas, N. A., Bodmeier, R. (2000). Bimodal drug release achieved with multi-layer matrix tablets: transport mechanisms and device design. *J. Control. Release*, *69*, 455–468.

Tahara, K., Yamamoto, K., & Nishihata, T. (1995). Overall mechanism behind matrix sustained release tablets prepared with hydroxypropyl methylcellulose 2910. *J. Control. Release*, *35*, 59–66.

The United States Pharmacopeia (2002). Chapters < 711 > and < 724 >, United States Pharmacopeial Convention, Inc.: Rockville, MD.

Wan, L. S. C., Heng, P. W. S., & Wong, L. F. (1995). Matrix swelling: a simple model describing extent of swelling of HPMC matrices. *Int. J. Pharm.*, *116*, 159–168.